Received: 2 April 2020 | Revised: 23 November 2020 | Accepted: 30 November 2020

Micro & Nano Letters

DOI: 10.1049/mna2.12038

The Institution of Engineering and Technology WILEY

LETTER

Effect of TiO_2 grain size on performance of $Ba_{0.5}Sr_{0.5}TiO_3$ based capacitors for energy storage application

1 | INTRODUCTION

The electrical energy storing capacity and holding capability are two major parameters of energy storage devices. The amount of stored electrical energy is directly related to capacitance and holding capability is inversely related to leakage current. Metal-insulator-metal (MIM) capacitor with suitable insulator material can achieve both of these properties. Barium strontium titanate ($Ba_{0.5}Sr_{0.5}TiO_3$) has high relative permittivity hence it is a good candidate for insulator material and can enhance specific capacitance (capacitance per unit mass) of MIM capacitor.

$Ba_{0.5}Sr_{0.5}TiO_3$ is a solid solution of barium titanate ($BaTiO_3$) and strontium titanate ($SrTiO_3$) and can be synthesized by many techniques such as hydrothermal [1, 2], solid-state reaction [3, 4], spray pyrolysis [5], sol-gel [6–8], RF magnetron sputtering [9, 10] and so on. $Ba_{0.5}Sr_{0.5}TiO_3$ is ferroelectric material having high dielectric constant, high breakdown field strength, low dielectric loss, pyroelectric properties, ferroelectricity and thermal stability and hence it is suitable for applications in ferroelectric random access memories (FRAM), multi-layer ceramic capacitors, tunable filters, microwave phase shifters, opto-electronic device, sensors [11–16].

The peculiar properties of $Ba_{0.5}Sr_{0.5}TiO_3$ make it suitable for considering in energy storage devices. Being a very good insulator, $Ba_{0.5}Sr_{0.5}TiO_3$ can be used as best candidate for insulator in metal–insulator–metal (MIM) capacitors which are electrostatic capacitors having fast charging- discharging characteristics and very high life–span.

In this work, $Ba_{0.5}Sr_{0.5}TiO_3$ nanopowder has been synthesized using barium carbonate ($BaCO_3$) and strontium carbonate ($SrCO_3$) as barium and strontium precursors, respectively. Commercially available titanium dioxide (TiO_2) and TiO_2 synthesized from titanium (Ti) isopropoxide were used as titanium precursors for $Ba_{0.5}Sr_{0.5}TiO_3$ nanopowder synthesis. Hence two $Ba_{0.5}Sr_{0.5}TiO_3$ nanopowder samples were synthesized. Further $Ba_{0.5}Sr_{0.5}TiO_3$ ceramic based MIM capacitor prepared from these two $Ba_{0.5}Sr_{0.5}TiO_3$ samples were fabricated with silver as top and bottom electrodes. The specific capacitance and the leakage current density are then evaluated and compared in this paper.

1.1 | Experimental

The $Ba_{0.5}Sr_{0.5}TiO_3$ nanopowder was first synthesized using $BaCO_3$ (American Chemical Society (ACS) reagent grade, 99%, Spectrum), $SrCO_3$ (ACS reagent grade, 99%, Spectrum) and TiO_2 (ACS reagent grade, 98%, Spectrum) as precursors for barium, strontium and titanium, respectively, which can be termed as BST1. In second sample (BST2), TiO_2 prepared from Ti isopropoxide was used for $Ba_{0.5}Sr_{0.5}TiO_3$ nanopowder synthesis. $Ba_{0.5}Sr_{0.5}TiO_3$ nanopowder synthesis of BST1 and BST2 samples are the same and is given in Figure 1.

The TiO_2 nanopowder for BST2 sample was synthesised from Ti isopropoxide, 0.1 molar sodium hydroxide (NaOH) solution and distilled water. Initially adequate distilled water in a beaker was placed over magnetic stirrer in fume cupboard. With continuous stirring added adequate Ti isopropoxide. Then added 0.1 molar NaOH solution till yellow colour of Ti isopropoxide solution turned to white. Further, the solution was heated in a sonicator for 30 m and then microwave irradiation was done at 350°C for 10 m. The solution is then kept for cooling down to room temperature normally. The sediment of the solution was obtained using a centrifuge and then the sediment was kept in a desiccator for 24 h.

The green pellets of BST1 and BST2 samples were made using Carver auto series NE pellet press after mixing BST samples with the binder (4 wt% aqueous polyvinyl alcohol (PVA)) and drying up in hot air oven at 60°C for 20 m. Further the pellets were sintered at 1275°C for 2 h in Nabertherm sintering furnace. After polishing, the thickness, diameter and mass of pellets were noted. Silver is coated on both sides of pellets for top and bottom electrodes for capacitors and dried in hot air oven at 130°C for 15 m.

The capacitance was measured using Hioki 3532-50 LCR Hi-Tester and the leakage current was measured at room temperature using Keithely IV meter. X-ray powder diffraction patterns were observed using Bruker D8 Advance equipment operating with Cu-Kα radiation (40 kV, 40 mA) at step of $2\theta = 0.02°$.

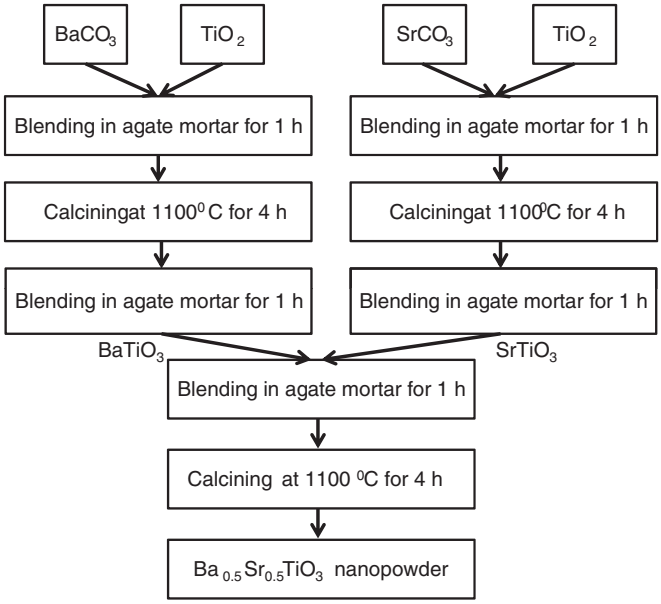

FIGURE 1 Process flow of synthesis of $Ba_{0.5}Sr_{0.5}TiO_3$ nanopowder

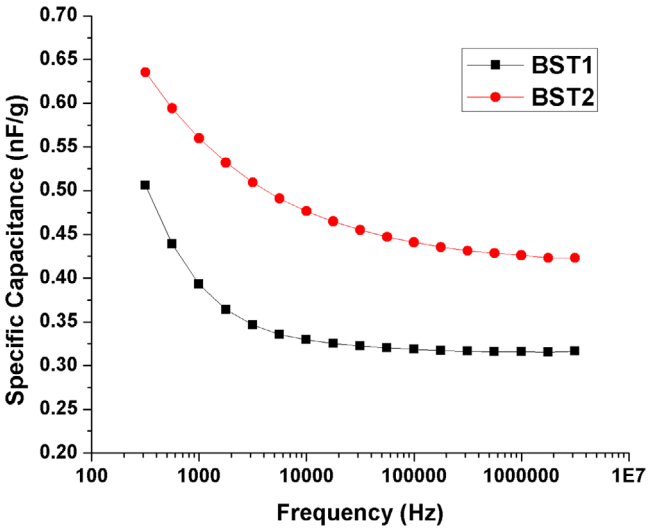

FIGURE 2 Specific Capacitance of $Ba_{0.5}Sr_{0.5}TiO_3$ ceramic based MIM capacitor

2 | RESULTS AND DISCUSSION

The performance comparison of BST1 and BST2 ceramics based Metal–Insulator–Metal capacitor is done in this section.

2.1 | Specific capacitance

The specific capacitance is relatively relevant performance parameter compared to capacitance density since the surface area of pellets when it undergo sintering. Figure 2 shows the specific capacitance of $Ba_{0.5}Sr_{0.5}TiO_3$ ceramic based MIM capacitor for BST1 and BST2 samples. It is evident from Figure 2 that $Ba_{0.5}Sr_{0.5}TiO_3$ ceramic based MIM capacitor synthesized using BST2 sample shows higher specific capacitance and is more suitable for storing more electrical energy.

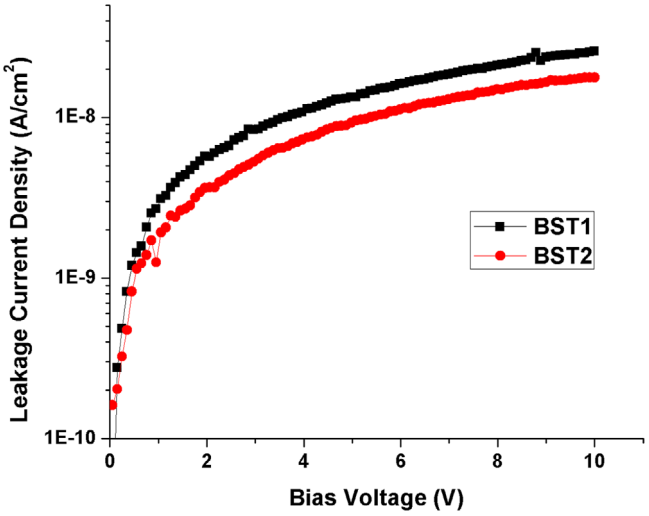

FIGURE 3 Leakage current density of $Ba_{0.5}Sr_{0.5}TiO_3$ ceramic based MIM capacitor

The specific capacitance of $Ba_{0.5}Sr_{0.5}TiO_3$ ceramic based MIM capacitors synthesized using BST1 and BST2 samples at 10 kHz frequency are observed as 0.33 nF/g and 0.48 nF/g, respectively. A specific capacitance enhancement of 45% is achieved in $Ba_{0.5}Sr_{0.5}TiO_3$ ceramic based MIM capacitor synthesized using BST2 sample. This enhanced energy storage capacity of $Ba_{0.5}Sr_{0.5}TiO_3$ ceramic based MIM capacitor synthesized using BST2 sample has a direct dependence on the mean crystallite size of synthesized TiO_2 and is explained in Section 3.3.

2.2 | Leakage current density

Figure 3 shows how leakage current density of $Ba_{0.5}Sr_{0.5}TiO_3$ ceramic based MIM capacitor using BST1 and BST2 samples varies with bias voltage. The leakage current density of $Ba_{0.5}Sr_{0.5}TiO_3$ ceramic based MIM capacitors synthesized using BST1 and BST2 samples at 1 V are observed as 2.91×10^{-9} A/cm^2 and 1.25×10^{-9} A/cm^2, respectively.

It is better to evaluate how the leakage current density varies with electric field than bias voltage owing to the difference in pellets' thickness. Leakage current density of $Ba_{0.5}Sr_{0.5}TiO_3$ ceramic based MIM capacitors using BST1 and BST2 samples is plotted against the electric field and is shown in Figure 4. 1 V bias corresponds to 5 V/cm electric field intensity owing to 2 mm mean thickness of pellets. The leakage current density of $Ba_{0.5}Sr_{0.5}TiO_3$ ceramic based MIM capacitors synthesized using BST1 and BST2 samples at 5 V/cm are observed as 3.48×10^{-9} A/cm^2 and 1.61×10^{-9} A/cm^2, respectively.

It is evident from Figures 3 and 4 that the leakage current performance of $Ba_{0.5}Sr_{0.5}TiO_3$ ceramic based MIM capacitor synthesized using BST2 sample is better than that synthesized using BST1 sample. A leakage current enhancement of 57%

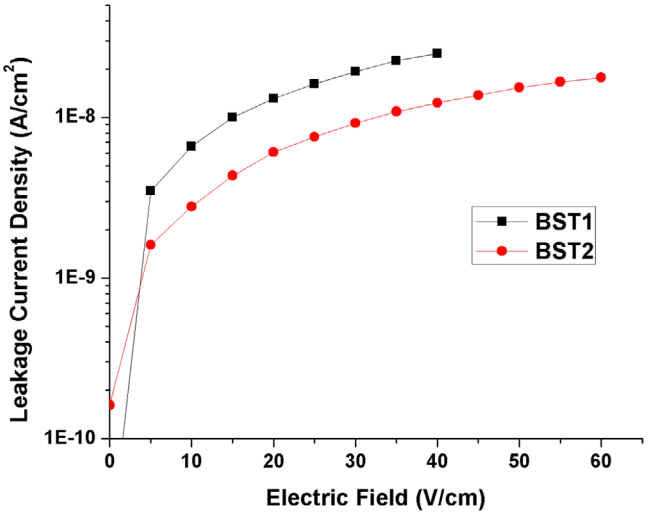

FIGURE 4 Leakage current density versus Electric field of $Ba_{0.5}Sr_{0.5}TiO_3$ ceramic based MIM capacitor

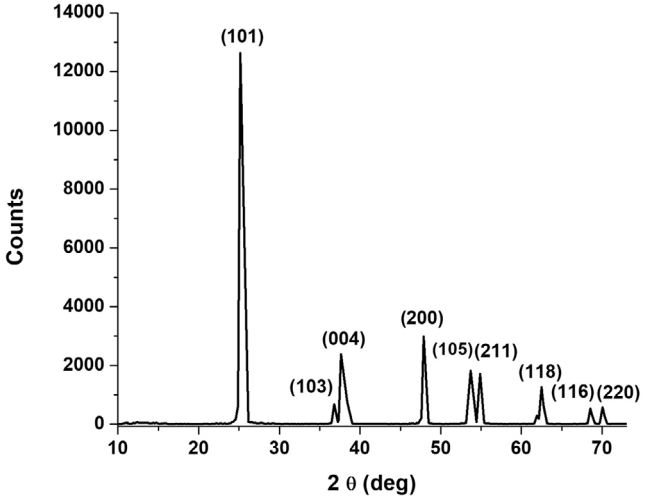

FIGURE 5 X-ray powder diffraction pattern of commercially available TiO_2 nanopowder

is achieved in $Ba_{0.5}Sr_{0.5}TiO_3$ ceramic based MIM capacitor synthesized using BST2 sample. Hence $Ba_{0.5}Sr_{0.5}TiO_3$ ceramic based MIM capacitor synthesized using BST2 sample is more suitable for holding stored electrical energy for longer duration and this performance enhancement is having direct dependence on crystallite size of synthesized TiO_2 nanopowder which is discussed in Section 3.3.

2.3 | X-ray powder diffraction

Figures 5 and 6 show X-ray powder diffraction patterns of commercially available TiO_2 nanopowder (ACS reagent grade, 98%, Spectrum) and synthesized TiO_2 nanopowder from Ti isopropoxide, respectively.

The diffraction peaks at angles 2θ = 25°, 36.8°, 37.7°, 48°, 54°, 55°, 63°, 69° and 70° which correspond to (101),

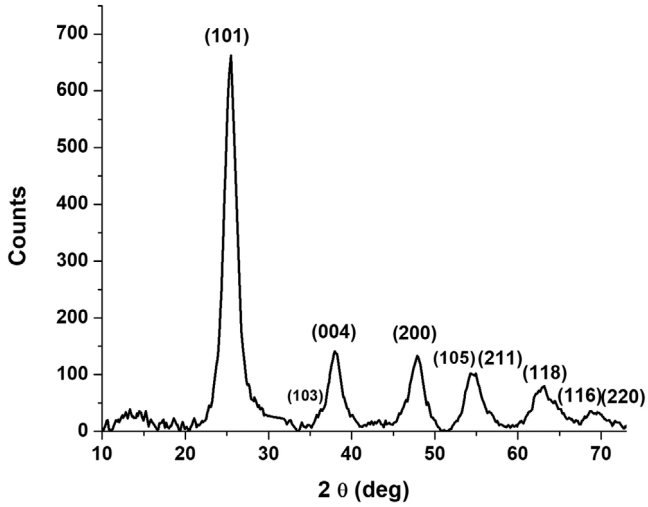

FIGURE 6 X-ray powder diffraction pattern of synthesized TiO_2 nanopowder

(103), (004), (200), (105), (211), (118), (116) and (220) planes of TiO_2, respectively [17, 18]. All diffraction peaks are in accord with the standard spectrum (JCPDS no. 84-1286) and which indicates that both the samples are in the anatase phase. The diffraction peaks of commercially available TiO_2 nanopowder are very sharp and having high intensities whereas that of synthesized TiO_2 nanopowder are broadened and having very low intensities. A strong diffraction peak is noted in both cases at a diffraction angle of 25° which corresponds to the plane (101) and is the dominant orientation of TiO_2.

The Debey-Scherrer equation [19] can be used to estimate crystallite size (grain size) from X-ray powder diffraction pattern. The lattice parameter can be computed using Bragg's law [20] and equation of cubic crystal [21]. The crystallite sizes and lattice parameters of commercially available TiO_2 nanopowder are given in Table 1 whereas that of synthesized TiO_2 nanopowder are given in Table 2.

The average grain size of commercially available TiO_2 nanopowder is 33 nm whereas that of synthesized TiO_2 nanopowder from Ti isopropoxide is 4 nm and hence achieved 88% reduction in grain size. This leads to a reduction in grain size of BST2 sample [8, 11, 12 16].

The lower grain size of BST2 sample is responsible for leakage current enhancement in $Ba_{0.5}Sr_{0.5}TiO_3$ ceramic based MIM capacitor synthesized using BST2 sample. Usually the measures for improving specific capacitance adversely affect leakage current [22]. It is evident from the results obtained in this work that the specific capacitance and leakage current together improve while using BST2 sample with low grain size for fabricating MIM capacitor.

The leakage current performance enhancement in MIM capacitor with BST2 sample of low grain size as insulator material is further investigated by X-ray powder diffraction pattern analysis of BST1 and BST2 samples. X-ray powder diffraction patterns of BST1 and BST2 nanopowder samples are given in Figure 7.

TABLE 1 Crystallite Size and Lattice Parameter of commercially available TiO_2 nanopowder at dominant planes of reflection using X-ray spectrum analysis

hkl	2θ (deg)	FWHM (deg)	d_{hkl} (A°)	Crystallite size (nm)	Lattice Parameter (A°)
101	25.171	0.211	3.535	38.167	4.999
103	36.813	0.220	2.439	37.651	4.878
004	37.658	0.228	2.386	36.420	4.773
112	38.426	0.224	2.341	37.156	4.682
200	47.888	0.260	1.897	33.074	3.795
105	53.728	0.274	1.704	32.152	4.175
211	54.898	0.283	1.671	31.293	4.093
118	62.508	0.290	1.484	31.699	4.695
116	68.561	0.346	1.367	27.486	3.868
220	70.080	0.335	1.341	28.650	3.794

TABLE 2 Crystallite Size and Lattice Parameter of synthesized TiO_2 nanopowder at dominant planes of reflection using X-ray spectrum analysis

hkl	2θ (deg)	FWHM (deg)	d_{hkl} (A°)	Crystallite size (nm)	Lattice Parameter (A°)
101	25.461	1.543	3.495	5.222	4.943
004	37.971	1.833	2.367	4.534	4.735
200	47.961	1.935	1.895	4.445	3.790
105	54.453	2.368	1.683	3.732	4.124
118	62.901	3.117	1.476	2.955	4.668

It is evident from Figure 7 that both BST1 and BST2 samples possess no secondary phases and it also indicates the formation of pure perovskite tetragonal structure. The characteristics peaks of BST2 nanopowder samples are sharper and of higher intensity compared to that of BST1 nanopowder sample. This accounts for the lower leakage current of MIM capacitor with BST2 sample of low grain size.

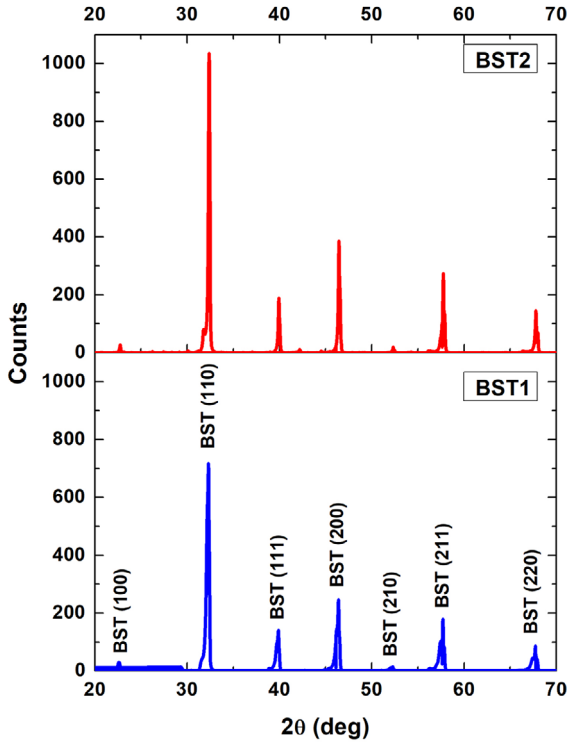

FIGURE 7 X-ray powder diffraction patterns of BST1 and BST2 nanopowder samples

2.4 | Series and leakage resistance

The capacitor can be modelled by its equivalent circuit which consists of the equivalent series resistor and equivalent series inductor in series with a capacitor; and leakage resistor in parallel with a capacitor. For better capacitance and leakage performance, equivalent series resistance (ESR) should be minimized and leakage resistance (R_p) should be maximized. ESR per unit mass versus frequency is shown in Figure 8 and R_p per unit mass versus frequency is shown in Figure 9.

From Figures 8 and 9, it is evident that $Ba_{0.5}Sr_{0.5}TiO_3$ ceramic based MIM capacitor synthesized using TiO_2 nanopowder with lower grain size shows lower ESR and higher R_p compared to $Ba_{0.5}Sr_{0.5}TiO_3$ ceramics based MIM capacitor synthesized using commercially available TiO_2 nanopowder. This modelling also justifies the performance enhancement of $Ba_{0.5}Sr_{0.5}TiO_3$ ceramic based MIM capacitor synthesized using TiO_2 nanopowder with lower grain size.

3 | CONCLUSION

$Ba_{0.5}Sr_{0.5}TiO_3$ nanopowder is synthesized using commercially available TiO_2 nanopowder (ACS reagent grade) and

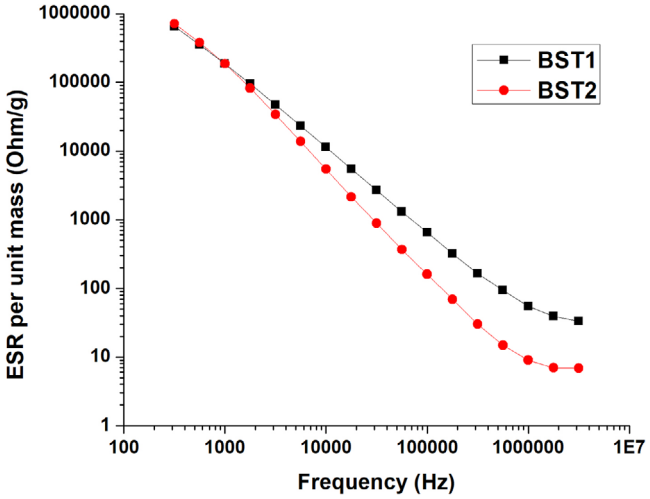

FIGURE 8 Equivalent series resistance (ESR) versus frequency of $Ba_{0.5}Sr_{0.5}TiO_3$ ceramic based MIM capacitor

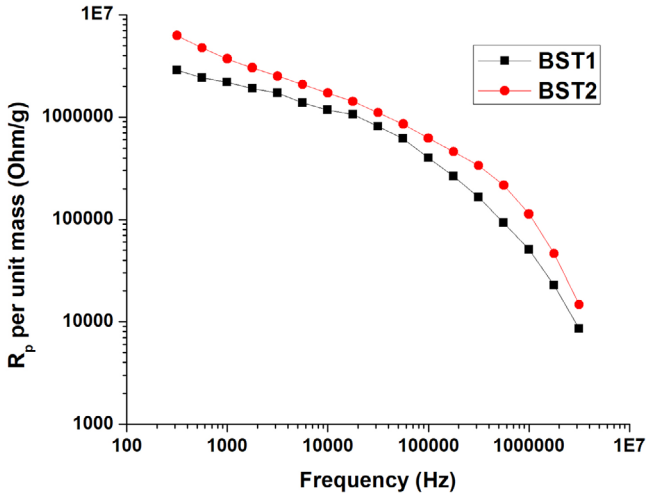

FIGURE 9 Leakage resistance (R_p) versus frequency of $Ba_{0.5}Sr_{0.5}TiO_3$ ceramic based MIM capacitor

synthesized TiO_2 nanopowder from Ti isopropoxide in this work. X-ray powder diffraction pattern analysis shows the changes in crystallinity and grain sizes of commercially available and synthesized TiO_2 nanopowder. The average grain size of commercially available TiO_2 nanopowder is 33 nm whereas that of synthesized TiO_2 nanopowder from Ti isopropoxide is 4 nm and hence achieved 88% reduction in grain size in TiO_2 nanopowder when synthesized from Ti isopropoxide. This leads to reduction in grain size of corresponding $Ba_{0.5}Sr_{0.5}TiO_3$ sample. Further the effect of grain size of TiO_2 on specific capacitance and leakage current density of $Ba_{0.5}Sr_{0.5}TiO_3$ ceramic based MIM capacitor are investigated. It is observed that $Ba_{0.5}Sr_{0.5}TiO_3$ ceramic based MIM capacitor synthesized using TiO_2 nanopowder with lower grain size shows higher specific capacitance as well as lower leakage current density. A 45% enhancement in specific capacitance and 57% enhancement in leakage current are achieved in $Ba_{0.5}Sr_{0.5}TiO_3$ ceramic based MIM capacitor synthesized using TiO_2 nanopowder with lower grain size. The lower leakage current of MIM capacitor with $Ba_{0.5}Sr_{0.5}TiO_3$ ceramic of low grain size is further investigated with its structure using X-ray powder diffraction pattern analysis as well. The $Ba_{0.5}Sr_{0.5}TiO_3$ ceramics synthesized using TiO_2 nanopowder with lower grain size is a suitable candidate for insulator material in MIM capacitors for energy storage application as it can store more electrical energy and can hold the stored energy for longer duration compared to $Ba_{0.5}Sr_{0.5}TiO_3$ ceramics synthesized using commercially available TiO_2 nanopowder.

The performance study of $Ba_{0.5}Sr_{0.5}TiO_3$ ceramic based MIM capacitor can be extended by tuning the grain size of TiO_2 nanopowder. The performance enhancement achieved with lower grain size insulator materials in this work, can be further investigated with barium strontium titanate with different barium mole fractions. In this work, all measurements have been done at room temperature. The effect of working temperature on the performance of $Ba_{0.5}Sr_{0.5}TiO_3$ ceramic based MIM capacitor can also be investigated.

ACKNOWLEDGEMENT

The authors are grateful to Dr. Surendran K.P. and his research team from CSIR-National Institute for Interdisciplinary Science and Technology (NIIST), Thiruvananthapuram, Kerala for help in making green pellets, sintering samples and capacitance measurements.

Smitha P. S.[1]
Jitha S. Jayan[2]
Saritha Appukuttan[2]
Suresh Babu V.[3]
Shiny G.[4]

[1] *Department of Electronics and Communication Engineering, College of Engineering Trivandrum, APJ Abdul Kalam Technological University, Kerala, India*
[2] *Department of Chemistry, Amrita School of Arts & Sciences, Amrita Vishwa Vidyapeetham, Amritapuri Campus, Kollam, Kerala, India*
[3] *Department of Electronics and Communication Engineering, Government Engineering College Wayanad, APJ Abdul Kalam Technological University, Kerala, India*
[4] *Department of Electronics and Communication Engineering, Government College of Engineering Kannur, APJ Abdul Kalam Technological University, Kerala, India*

Correspondence
P. S. Smitha, Department of Electronics and Communication Engineering, College of Engineering Trivandrum, APJ Abdul Kalam Technological University, Kerala, India.
Email: smithaps@cet.ac.in

REFERENCES

1. Zhu, J., et al.: Resistive switching characteristics of resistive random access memory based on a $Ba_xSr_{1-x}TiO_3$ thin film grown by a hydrothermal method. IEEE Ele. Dev. Lett. 40(9), 1411–1414 (2019)

2. Jin, Q., et al.: Microstructure, dielectric properties and energy storage performance of $Ba_{0.4}Sr_{0.6}TiO_3$ ceramics prepared by hydrothermal method and microwave sintering. Mater. Lett. 188, 159–161 (2017)
3. Sandi, D.K., et al.: The influences of mole composition of strontium on properties of barium strontium titanate ($Ba^{1-x}Sr_xTiO_3$) prepared by solid state reaction method. AIP Conf. Proc. 1710, 1, 030006 (2016)
4. Shen, Z.Y., et al.: Glass modified barium strontium titanate ceramics for energy storage capacitor at elevated temperatures. J. Materiomics 5(4), 641–648 (2019)
5. Tetsi, E., et al.: $Ba_{0.6}Sr_{0.4}TiO_3$ thin films deposited by spray coating for high capacitance density capacitors. Phys. Status Solidi. A 215(23), 1800478 (2018)
6. Debnath, A., Srivastava, V., Singh, S.: Sol-gel derived BST ($Ba_xSr_{1-x}TiO_3$) thin film ferroelectrics for non-volatile memory application with metal-ferroelectric-semiconductor (MFS) structure. Appl. Nanosci. 10(12), 5511–5521 (2020)
7. Bakar, N.A., et al.: Sol gel preparation methods for barium strontium titanate based solar devices. AIP Conf. Proc. 2068, 1, 020057 (2019)
8. Batttisha, I.K., et al.: Structural, magnetic and dielectric properties of Fe-Co Co-doped $Ba_{0.9}Sr_{0.1}TiO_3$ prepared by sol gel technique. New J. Glass Ceram. 4, 19–28 (2014)
9. Li, J., et al.: Radio frequency (RF) magnetron sputtered barium strontium titanate (BST) thin film. Key Eng. Mater. 727, 942–946 (2017)
10. Gao, F., An, J.: BST thin films deposited by RF-magnetron sputtering and dielectric property research. In: IEEE Advanced Information Management, Communicates, Electronic and Automation Control Conf. (IMCEC), pp. 1808–1811 (2016)
11. Araghi, M.A., Shaban, N., Bahar, M.: Synthesis and characterization of nanocrystalline barium strontium titanate powder by a modified sol-gel processing. Mater. Sci.-Poland 34(1), 63–68 (2016)
12. Attar, A.S., Sichani, E.S., Sharafi, S.: Structural and dielectric properties of Bi-doped barium strontium titanate nanopowders synthesized by sol-gel method. J. Mater. Res. and Technol. 6(2), 108–115 (2017)
13. Cai, W., et al.: Vanadium doping effects on microstructure and dielectric properties of barium titanate ceramics. Ceram. Int. 37(8), 3643–3650 (2011)
14. Gao, Y., et al.: Nanocrystalline barium strontium titanate ceramics synthesized via the organosol route and spark plasma sintering. J. Amer. Ceram. Soc. 97(7), 2139–2146 (2014)
15. Olhero, S.M., Kaushal, A., Ferreira, J.M.: Fabrication of barium strontium titanate ($Ba_{0.6}Sr_{0.4}TiO_3$) 3D microcomponents from aqueous suspensions. J. Amer. Ceram. Soc. 97(3), 725–732 (2014)
16. Balachandran, R., et al.: Phase formation and dielectric properties of $Ba_{0.5}Sr_{0.5}TiO_3$ by slow injection sol-gel technique. J. Mater. Sci. 46(6), 1806–1813 (2011)
17. Kibasomba, P.M., et al.: Strain and grain size of TiO_2 nanoparticles from TEM, Raman spectroscopy and XRD: The revisiting of the Williamson-Hall plot method. Resul. Phys. 9, 628–635 (2018)
18. Vorontsov, A.V., Tsybulya, S.V.: Influence of nanoparticles size on XRD patterns for small monodisperse nanoparticles of Cu° and TiO_2 anatase. Indust. Eng. Chem. Res. 57(7), 2526–2536 (2018)
19. Lin, D.Y., et al.: Nanorod arrays enhanced UV light response of Mg-doped ZnO films. Symmetry 12(6), 1005 (2020)
20. Greenberg, B.: Bragg's law with refraction. Acta Crystallographica Sec. A: Found. of Crystallo. 45(3), 238–241 (1989)
21. Kaszkur, Z.: Nanopowder diffraction analysis beyond the Bragg law applied to palladium. J. Appl. Crystallo. 33(1), 87–94 (2000)
22. Smitha, P.S., Suresh Babu, V., Shiny, G.: Critical parameters of high performance metal–insulator–metal nanocapacitors: A review. Mater. Res. Expr. 6(12), 122003 (2019)